

Optimization of a reversed trapezoidal fin using a 2-D analytic method

Hyung Suk Kang*

Division of Mechanical and Mechatronics Engineering, Kangwon National University,
Hyoza-dong, Chuncheon, Kangwon-do, 200-701, Korea

(Manuscript Received June 19, 2007; Revised October 8, 2007; Accepted October 9, 2007)

Abstract

A reversed trapezoidal fin with variable fin base thickness is optimized based on the fixed fin volume by using a two-dimensional analytic method. The variation of temperature along the normalized Y position at the fin tip is presented. For fixed fin volumes, the maximum heat loss, the corresponding optimum fin effectiveness, fin base height and fin tip length as a function of the fin base thickness, fin shape factor and the fin volume are presented. One of the results shows that both the optimum heat loss and the optimum fin length increase with the increase of the value of fin shape factor.

Keywords: Optimization; Fin base thickness; Fin shape factor; Convection characteristic number

1. Introduction

Extended surfaces or fins are widely used to increase heat dissipation between a solid surface and its adjoining fluid in many engineering and industrial applications such as the cooling of combustion engines, electronic equipment, many kinds of heat exchangers, and so on. As a result, a great deal of attention has been directed to fin problems and many studies on various shapes of fins have been presented. The most commonly studied fins are longitudinal rectangular, triangular, trapezoidal fins and the annular or circular fins. For example, the rate of heat loss from a rectangular fin governed by the power law-type temperature dependence was studied [1] while heat conduction in an array of triangular fins with an attached wall was analyzed by the finite element method [2]. An analysis of the heat transfer characteristics of a circular fin dissipating heat from its surface by convection and radiation was made [3].

The optimum procedure for fin shapes is of great interest for many engineering topics. For common fin

shapes, the optimum dimensions of rectangular fins and cylindrical pin fins were investigated [4]. The optimization of rectangular profile circular fins with variable thermal conductivity and convective heat transfer coefficients was discussed [5]. The optimization of a convective and radiating annular fin under thermally asymmetric condition was reported [6].

Also, optimization of the unique shape of the fin has been presented. For this kind of paper, Bejan and Almogbel [7] reported the geometric (constructal) optimization of T-shaped fin assemblies, where the objective is to maximize the global conductance of the assembly, subject to total volume and fin-material constraints. Recently, elliptical disk fins were analyzed and optimized using a semi-analytical technique [8]. In these optimum procedures for the unique fin shape, fin base temperature is given as a constant for the fin base boundary condition.

In this study, the optimization of a reversed trapezoidal fin with various fin lateral surface slopes is presented for fixed fin volumes using a two-dimensional analytic method. This two-dimensional analytic method has been compared with many numerical methods and experimental results and has been shown to have very good agreement with those

*Corresponding author. Tel.: +82 33 250 6316, Fax.: +82 33 242 6013
E-mail address: hkang@kangwon.ac.kr
DOI 10.1007/s12206-007-1038-1

results. For example, the temperature profile along the triangular fin center line calculated by the finite element method [2] was exactly the same as that obtained by the analytic method [9]. A comparison between the analytic method and finite difference method was made for a trapezoidal fin [10]. Also, for a trapezoidal fin, the experimental results for the temperature and heat loss were compared and shown to be good in agreement with those obtained from the analytic method [11], and both results were shown to be in good agreement. In this study, both the fin base thickness and base height can be variable. Therefore, the thermal resistance from the inside wall to the fin base and the fin base temperature can be changed due to the variations of the fin base thickness and base height.

2. 2-D Analytical methods

A schematic diagram of a reversed trapezoidal fin is shown in Fig. 1. In this diagram, the fin lateral surface slope s is denoted by $l_h(1-\xi)/(l_e-l_b)$ and the shape of the fin becomes rectangular for $\xi=1$ and that becomes the reversed trapezoidal fin for which the tip height is twice the base height in the case of $\xi=0$. For this schematic diagram, the dimensionless two-dimensional governing differential equation under steady state is

$$\frac{\partial^2 \theta}{\partial X^2} + \frac{\partial^2 \theta}{\partial Y^2} = 0. \quad (1)$$

One energy balance condition and three boundary conditions are required to solve the governing differential equation and these conditions are given as Eqs. (2)-(5).

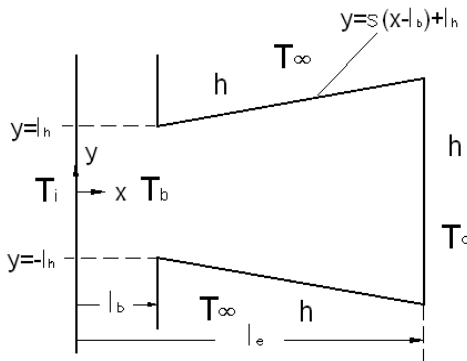


Fig. 1. Geometry of a reversed trapezoidal fin.

$$\left. \frac{\partial \theta}{\partial X} \right|_{X=L_b} + \frac{1-\theta|_{X=L_b}}{L_b} = 0 \quad (2)$$

$$\left. \frac{\partial \theta}{\partial Y} \right|_{Y=0} = 0 \quad (3)$$

$$\left. \frac{\partial \theta}{\partial X} \right|_{X=L_e} + M \cdot \theta|_{X=L_e} = 0 \quad (4)$$

$$\begin{aligned} & - \int_0^{L_h} \left. \frac{\partial \theta}{\partial X} \right|_{X=L_b} dY \\ & = M \cdot \int_{L_h}^{s(L_e-L_b)+L_h} \theta \sqrt{(1/s)^2 + 1} dY \\ & - \int_0^{s(L_e-L_b)+L_h} \left. \frac{\partial \theta}{\partial X} \right|_{X=L_e} dY \end{aligned} \quad (5)$$

For a rectangular fin case (i.e., $\xi=1$ or $s=0$), Eq. (5) for the energy balance condition is replaced by Eq. (6) for the fin top boundary condition.

$$\left. \frac{\partial \theta}{\partial Y} \right|_{Y=L_h} + M \cdot \theta|_{Y=L_h} = 0 \quad (6)$$

When Eq. (1) with three boundary conditions (2), (3) and (4) is solved by using the separation of variables procedure, the temperature distribution $\theta(X, Y)$ within the reversed trapezoidal fin can be obtained. The result is

$$\theta(X, Y) = \sum_{n=1}^{\infty} \frac{g_1(\lambda_n) \cdot f(X) \cdot \cos(\lambda_n Y)}{g_2(\lambda_n) + g_3(\lambda_n)}. \quad (7)$$

where,

$$f(X) = \cosh(\lambda_n X) + g_4(\lambda_n) \cdot \sinh(\lambda_n X) \quad (8)$$

$$g_1(\lambda_n) = \frac{4 \sin(\lambda_n L_h)}{2 \lambda_n L_h + \sin(2 \lambda_n L_h)} \quad (9)$$

$$g_2(\lambda_n) = \cosh(\lambda_n L_b) - L_b \cdot \lambda_n \cdot \sinh(\lambda_n L_b) \quad (10)$$

$$g_3(\lambda_n) = g_4(\lambda_n) \cdot \{ \sinh(\lambda_n L_b) - L_b \cdot \lambda_n \cdot \cosh(\lambda_n L_b) \} \quad (11)$$

$$g_4(\lambda_n) = - \frac{\lambda_n \cdot \tanh(\lambda_n L_e) + M}{\lambda_n + M \cdot \tanh(\lambda_n L_e)} \quad (12)$$

The eigenvalues λ_n can be obtained from Eq. (13) which is an arranged form of Eq. (5).

$$0 = g_5(\lambda_n) - g_6(\lambda_n) + g_7(\lambda_n)[\{g_8(\lambda_n) + g_9(\lambda_n)\} \cdot \{g_{10}(\lambda_n) + g_{11}(\lambda_n) - g_{12}(\lambda_n) - g_{13}(\lambda_n)\} + \{g_{14}(\lambda_n) + g_{15}(\lambda_n)\} \cdot \{g_{16}(\lambda_n) + g_{17}(\lambda_n) - g_{18}(\lambda_n) - g_{19}(\lambda_n)\}] \quad (13)$$

where,

$$\begin{aligned} g_5(\lambda_n) &= \{\sinh(\lambda_n L_b) + g_4(\lambda_n) \cdot \cosh(\lambda_n L_b)\} \\ &\quad \sin(\lambda_n L_h) \end{aligned} \quad (14)$$

$$\begin{aligned} g_6(\lambda_n) &= \{\sinh(\lambda_n L_e) + g_4(\lambda_n) \cdot \cosh(\lambda_n L_e)\} \\ &\quad \sin\{(\lambda_n(2-\xi)L_h)\} \end{aligned} \quad (15)$$

$$g_7(\lambda_n) = M / (\lambda_n \cdot \sqrt{1+s^2}) \quad (16)$$

$$g_8(\lambda_n) = \cosh\{\lambda_n(L_b - \frac{L_h}{s})\} \quad (17)$$

$$g_9(\lambda_n) = g_4(\lambda_n) \cdot \sinh\{\lambda_n(L_b - \frac{L_h}{s})\} \quad (18)$$

$$g_{10}(\lambda_n) = \sinh\{\frac{\lambda_n}{s}(2-\xi)L_h\} \cdot \cos\{\lambda_n(2-\xi)L_h\} \quad (19)$$

$$g_{11}(\lambda_n) = s \cdot \cosh\{\frac{\lambda_n}{s}(2-\xi)L_h\} \cdot \sin\{\lambda_n(2-\xi)L_h\} \quad (20)$$

$$g_{12}(\lambda_n) = \cos(\lambda_n L_h) \sinh(\frac{\lambda_n L_h}{s}) \quad (21)$$

$$g_{13}(\lambda_n) = s \cdot \sin(\lambda_n L_h) \cosh(\frac{\lambda_n L_h}{s}) \quad (22)$$

$$g_{14}(\lambda_n) = \sinh\{\lambda_n(L_b - \frac{L_h}{s})\} \quad (23)$$

$$g_{15}(\lambda_n) = g_4(\lambda_n) \cosh\{\lambda_n(L_b - \frac{L_h}{s})\} \quad (24)$$

$$g_{16}(\lambda_n) = \cosh\{\frac{\lambda_n}{s}(2-\xi)L_h\} \cdot \cos\{\lambda_n(2-\xi)L_h\} \quad (25)$$

$$g_{17}(\lambda_n) = s \cdot \sinh\{\frac{\lambda_n}{s}(2-\xi)L_h\} \cdot \sin\{\lambda_n(2-\xi)L_h\} \quad (26)$$

$$g_{18}(\lambda_n) = \cos(\lambda_n L_h) \cosh(\frac{\lambda_n L_h}{s}) \quad (27)$$

$$g_{19}(\lambda_n) = s \cdot \sin(\lambda_n L_h) \sinh(\frac{\lambda_n L_h}{s}) \quad (28)$$

The eigenvalues λ_n can be calculated by using Eq. (29) which is derived from Eq. (6) for a rectangular fin case.

$$\lambda_n \cdot \tan(\lambda_n) = M \quad (29)$$

The heat loss conducted into the fin through the fin base is calculated by

$$q = -2 \int_0^{l_h} k \frac{\partial T}{\partial x} \Big|_{x=l_b} l_w dy. \quad (30)$$

Then, the dimensionless heat loss from the reversed trapezoidal fin is obtained by using Eq. (31).

$$Q = \frac{q}{k \varphi_i l_w} = -2 \sum_{n=1}^{\infty} \frac{g_1(\lambda_n) \cdot g_5(\lambda_n)}{g_2(\lambda_n) + g_3(\lambda_n)} \quad (31)$$

If there is no temperature gradient in the y and z directions between the inside wall and outside bare wall for the range of $-l_h < y < l_h$ in the no fin case, the dimensionless heat loss from the outside bare wall is given as Eq. (32).

$$Q_w = \frac{q_w}{k \varphi_i l_w} = \frac{2M \cdot L_h}{1 + M \cdot L_b} \quad (32)$$

Fin effectiveness is then expressed as

$$\varepsilon = \frac{Q}{Q_w}. \quad (33)$$

The reversed trapezoidal fin volume, as shown in Fig. 1, can be calculated by Eq. (34) and the arranged dimensionless fin volume is given by Eq. (35).

$$V = 2l_w \int_{l_b}^{l_e} s(x \cdot l_b) + l_b dx \quad (34)$$

$$V = \frac{V}{l_c^2 \cdot l_w} = (3-\xi)L_h(L_e - L_b) \quad (35)$$

The fin surface area with assuming $l_w \gg 2l_h$ is presented by Eq. (36) and the dimensionless form is written by Eq. (37).

$$a = [2\sqrt{(l_e - l_b)^2(1+s^2)} + 2\{s(l_e - l_b) + l_h\}] \cdot l_w \quad (36)$$

$$\begin{aligned} A &= \frac{a}{l_c \cdot l_w} \\ &= 2\sqrt{(L_e - L_b)^2 + \{(1-\xi)L_h\}^2} + 2(2-\xi)L_h \end{aligned} \quad (37)$$

3. Results and discussions

For three different fin base height values, the temperature profile along the normalized Y position at the fin tip [i.e., $NY=Y/\{(2-\xi)L_h\}$] is represented in Fig. 2. The normalized Y position at the fin tip NY is given as $Y/(1.5L_h)$ for $\xi=0.5$ so that $NY=0$ represents the center position and $NY=1$ represents the top position. It can be noted that the variation of temperature along the NY becomes more remarkable as the fin base height increases from 0.5 to 1.0, and this phenomenon is more obvious in the case of $L_e=1$ and $M=0.3$. The condition for $\xi=0.75$, $L_b=0.1$, $L_h=0.1$, $L_e=1$ and $M=0.1$, which is not shown in Fig. 2 in this study, is almost the same as the condition for $\xi=0.75$, $L_b=1.1$, $L_h=0.1$, $L_e=2$, $M=0.1$ and $M_f=1000$ that is given in Table 1 in the reference [12]. When the temperatures between these two conditions are compared, the value of $\theta(L_b)=0.9267$ given in Table 1 in the reference [12] is within the values of $\theta(L_b, 0)=0.9295$, $\theta(L_b, 0.05)=0.9287$ and $\theta(L_b, 0.1)=0.9258$ in the present study.

Table 1 lists the variation of the fin base temperature as a function of fin base thickness, base height and the convection characteristic number. It can be noted that the fin base temperature increases as the

Table 1. Variation of the fin base temperature ($L_e-L_b=1.5$, $\xi=0.5$, $y=0$).

L_b	$\theta _{X=L_b}$			
	$L_h=0.05$		$L_h=0.2$	
	$M=0.01$	$M=0.1$	$M=0.01$	$M=0.1$
0.1	0.9736	0.8792	0.9917	0.9447
0.01	0.9973	0.9866	0.9992	0.9944
0.001	0.9997	0.9987	0.9999	0.9994

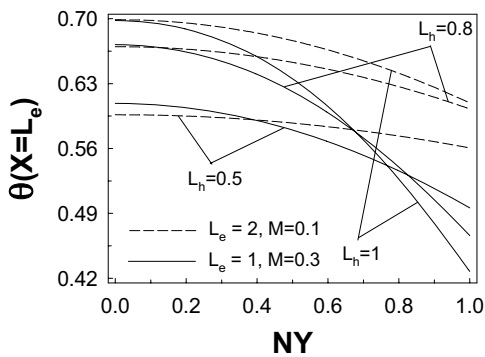


Fig. 2. Dimensionless temperature profile along the normalized position of Y ($\xi=0.5$, $L_b=0.1$).

convection characteristic number and base thickness decrease or as the base height increases. Physically, the value of the fin base temperature should approach the inner wall temperature (i.e., $\theta=1$) as the fin base thickness approaches 0, and this trend is illustrated well in this table.

The dimensionless heat loss as a function of the fin length for different values of the fin base thickness in the case of fixed fin volume is presented in Fig. 3. It is observed that the heat loss increases rapidly when the fin length approaches fin base thickness (i.e. very short fin). It is because the fin base height will increase as the fin length decreases for a fixed fin volume. Obviously, the design in this case is impractical, although the heat dissipation is large. Another important phenomenon shown in Fig. 3 is that the maximum heat loss does not exist at the practical fin length when the fin base thickness is beyond a certain value. For example, the maximum heat loss exists for $L_b=0.01$ and $L_b=0.1$, whereas it does not exist for $L_b=0.3$. The maximum heat loss will be referred to as the optimum heat loss and the variables at which the maximum heat loss exists are referred to as the optimum variables in this paper.

Fig. 4 depicts the variation of the optimum heat loss and fin effectiveness as a function of the fin base thickness for a reversed trapezoidal fin when the dimensionless fin volume is arbitrarily fixed as 0.5. The optimum effectiveness means the effectiveness when the heat loss becomes the maximum heat loss for given conditions. This figure indicates that both the optimum heat loss and corresponding optimum fin effectiveness decrease with the increase of the fin base thickness. It can be noted that the optimum heat loss increases while the corresponding optimum

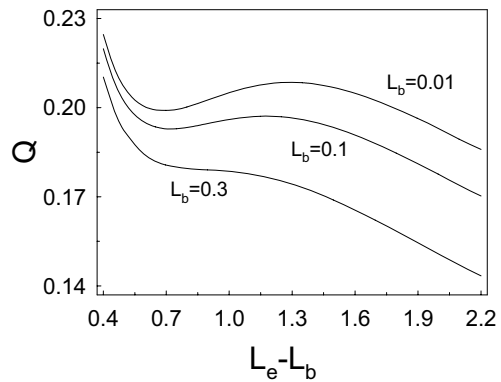


Fig. 3. Heat loss as a function of the fin length for the fixed fin volume ($\xi=0.5$, $M=0.1$, $V=0.5$).

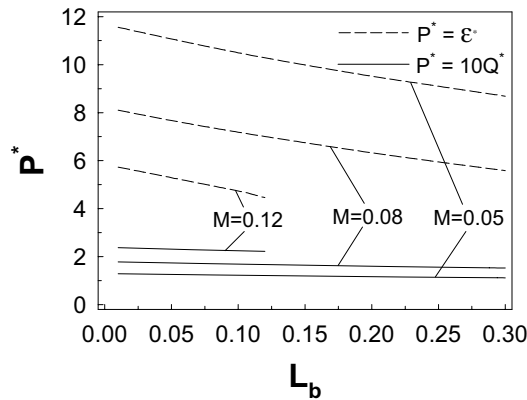


Fig. 4. Optimum heat loss and fin effectiveness versus the fin base thickness ($\xi = 0.5$, $V=0.5$).

effectiveness decreases as the convection characteristic number increases for the same value of fin base thickness.

Fig. 5 presents the variation of the optimum fin length and base height under the same condition as given in Fig. 4. It is shown that the optimum fin length decreases monotonically and the optimum fin base height increases due to the fixed volume with the increase of fin base thickness. Physically, it means that the optimum fin shape becomes shorter and fatter as the fin base thickness increases. It also shows that the optimum fin base height increases while the optimum fin length decreases as the convection characteristic number increases for the same value of fin base thickness. To illustrate how to transform dimensionless data to the practical application, $L_e^* - L_b = 1.351$ and $L_h^* = 0.148$ for $L_b = 0.1$ and $M = 0.08$ from Fig. 5 are considered as an example. The value of h is arbitrarily chosen to be $200 \text{ W/m}^2\text{C}$ for forced convection condition of some gases, and k is given as $52 \text{ W/m}\text{C}$ for commercial bronze (90% Cu, 10% Al). Then l_c becomes about 2cm and the practical optimum fin tip length is $1.351 \times 2\text{cm} = 2.70\text{cm}$, and the optimum half fin height is $0.148 \times 2\text{cm} = 0.296\text{cm}$.

Though the fin shape factor, ξ , is usually chosen for fin fabricating convenience, it is worthwhile to explore its effect on the optimum designs. As already mentioned, $\xi = 1$ means the rectangular fin and $\xi = 0$ presents the reversed trapezoidal fin for which the fin tip height is twice the fin base height. In Fig. 6, it is seen that, for the same volume, the optimum heat loss increases as ξ increases for all three values of M . However, the corresponding optimum effectiveness

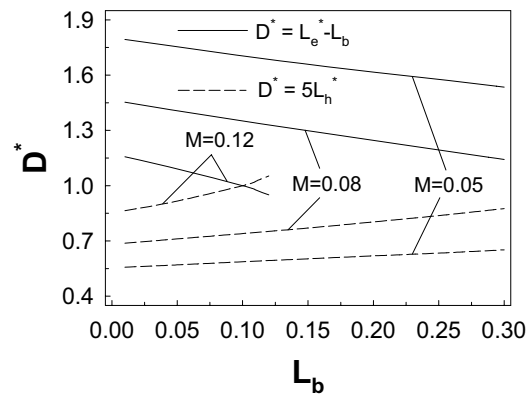


Fig. 5. Optimum fin length and fin base height versus the fin base thickness ($\xi = 0.5$, $V=0.5$).

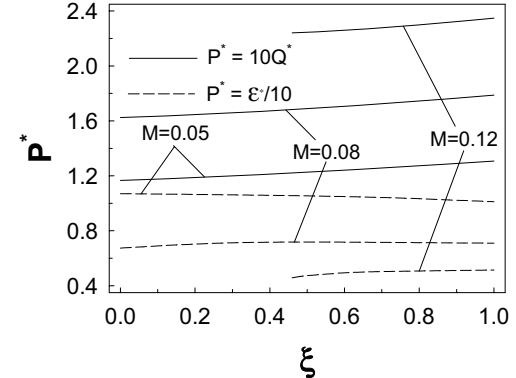


Fig. 6. Optimum heat loss and fin effectiveness versus the fin shape factor ($V=0.5$, $L_b=0.1$).

continuously increases for $M=0.12$ and that increases first and then decreases for $M=0.08$, while that monotonically decreases for $M=0.05$ with the increase of the fin shape factor.

Fig. 7 shows the optimum fin tip length and fin base height as a function of the fin shape factor under the same condition as given in Fig. 6. It shows that the optimum fin tip length increases almost linearly, while the variation of the optimum fin base height is not much with the increase of ξ . This phenomenon explains why the optimum heat loss increases with the increase of ξ for the fixed fin volume as already shown in Fig. 6. Physically, it also means that, if the dimensionless fin volume V is the same, the optimum rectangular fin is always longer than the optimum reversed trapezoidal fin.

Table 2 lists the relative increasing rate of the optimum dimensions for the cases of $M=0.05$ and 0.08 as shown in Fig. 7. Both the increasing rates of the

Table 2. Relative I.R. (%) of the optimum dimensions ($V=0.5$, $L_b=0.1$).

ξ	$\frac{L_e^*(\xi) - L_e^*(\xi = 0)}{L_e^*(\xi = 0)}$		$\frac{L_h^*(\xi) - L_h^*(\xi = 0)}{L_h^*(\xi = 0)}$	
	M=0.05	M=0.08	M=0.05	M=0.08
0.25	5.55	11.69	3.01	-3.23
0.5	11.72	21.12	6.66	-2.50
0.75	18.01	29.63	11.86	0.72
1.0	24.86	39.90	18.52	4.48

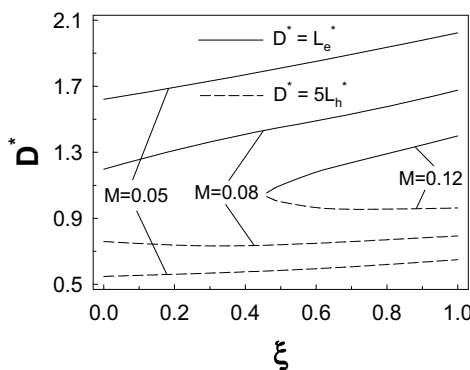


Fig. 7. Optimum fin tip length and fin base height versus the fin shape factor ($V=0.5$, $L_b=0.1$).

optimum fin tip length and fin base height increase as ξ increases in the case of $M=0.05$. Even though the increasing rate of the optimum fin base height decreases slightly first and then increases slightly, that of the optimum fin tip length is remarkable with the increase of ξ for $M=0.08$. Probably due to these phenomena, the optimum heat loss increases with the increase of ξ .

The dimensionless fin volume, V , was arbitrarily selected to be 0.5 in the previous discussion. The variations of the optimum heat loss and effectiveness as a function of V are shown in Fig. 8. As expected, the increase of V enhances the optimum heat loss. It also shows that the corresponding optimum effectiveness decreases somewhat rapidly first and then decreases slowly as the fin volume increases from 0.1 to 1.

Fig. 9 represents the optimum dimensions versus the fin volume for the same condition as given in Fig. 8. It shows that the optimum fin tip length increases somewhat rapidly first and then levels off for $M=0.05$ and 0.08, while that increases first and then decreases slightly for $M=0.12$ with the increase of the fin volume. Also, the optimum fin base height increases

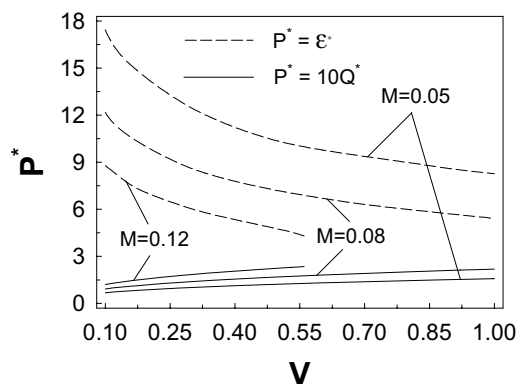


Fig. 8. Optimum heat loss and fin effectiveness versus the fin volume ($\xi = 0.5$, $L_b = 0.1$).

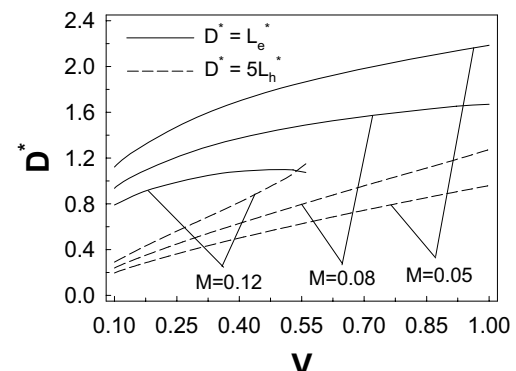


Fig. 9. Optimum fin tip length and fin base height versus the fin volume ($\xi = 0.5$, $L_b = 0.1$).

monotonically with the increase of total fin volume. Physically, the optimum reversed trapezoidal profile fin becomes rather ‘fatter’ with the increase of the fin volume.

The convection characteristic numbers were arbitrarily chosen to be 0.08, 0.1 and 0.12 in the previous discussion. The variations of the optimum heat loss and effectiveness as a function of M are presented in Fig. 10. The optimum heat loss increases almost monotonically as M increases from 0.001 to 0.1. It also shows that the corresponding optimum effectiveness decreases very rapidly as M decreases from 0.001 to about 0.01, and then decreases somewhat slowly as M decreases from about 0.01 to 0.1. The fin is thus remarkably useful under natural convection conditions.

Fig. 11 presents the variation of the optimum fin length and base height under the same condition as given in Fig. 10. The optimum fin length decreases remarkably as M increases from 0.001 to 0.01 and

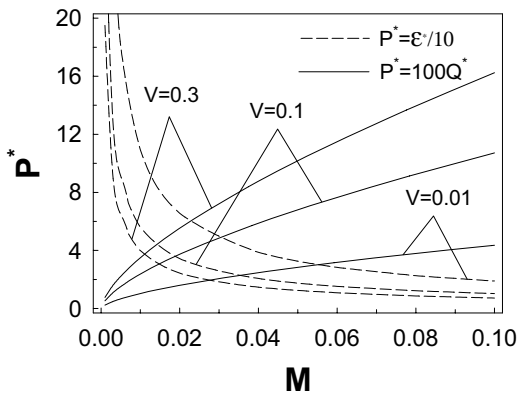


Fig. 10. Optimum heat loss and fin effectiveness versus the convection characteristic number ($\xi = 0.5$, $L_b = 0.1$).

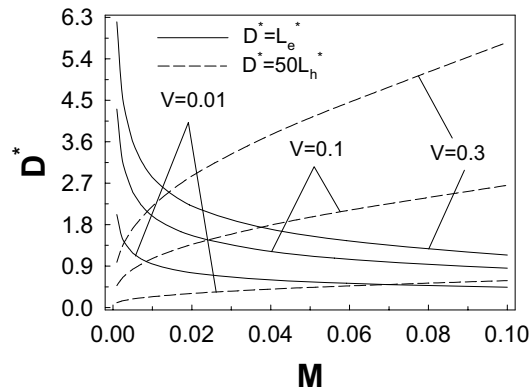


Fig. 11. Optimum fin tip length and fin base height versus the convection characteristic number ($\xi = 0.5$, $L_b = 0.1$).

then decreases somewhat slowly as M increases from 0.01 to 0.1. The base height increases as the fin length decreases due to the fixed fin volume. As one more example for the practical dimension under a free convection condition, $L_e^* = 4.31$ and $L_h^* = 0.0095$ for $V=0.1$ and $M=0.001$ from Fig. 11 are considered. The value of l_c is arbitrarily chosen to be 2.5cm and k is given as 401 W/m°C for pure copper. Then h is 16.04 W/m²°C for free convection of some gases and the practical optimum fin tip length is $4.31 \times 2.5\text{cm} = 10.78\text{cm}$ and the optimum half fin height is $0.0095 \times 2.5\text{cm} = 0.024\text{cm}$.

The dimensionless heat loss as a function of fin length for different values of the fin base thickness in the case of fixed fin surface area is presented in Fig. 12. It is observed that the heat loss increases very rapidly and reaches the maximum value and then decreases somewhat rapidly with the increase of the fin length for all three values of the fin base thickness.

Table 3. Ratio of the optimum fin tip length to base height for fixed fin surface area ($\xi = 0.5$, $L_b = 0.1$).

M	$L_e^*/(2L_h^*)$ (%)		
	A=2	A=3	A=4
0.01	29.82	25.61	23.76
0.04	29.44	25.28	23.28
0.08	29.19	24.88	22.59
0.1	28.94	24.55	22.23

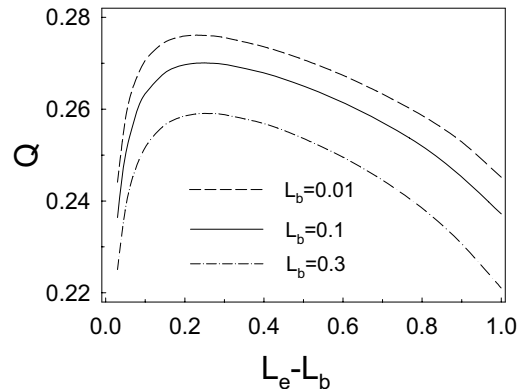


Fig. 12. Heat loss as a function of the fin length for the fixed fin surface area ($\xi = 0.5$, $L_b = 0.1$, $A=3$).

There are two distinct differences between the fixed volume case and the fixed surface area case. First, the variation trend of the heat loss with the variation of the fin length is different. Second, the fin length for the maximum heat loss in the case of fixed fin surface area is relatively very short compared to that in the case of fixed fin volume.

Table 3 lists the ratio of the optimum fin tip length to base height for fixed fin surface areas with the variation of the convection characteristic number and the fixed surface area. The ratio decreases as the convection characteristic number and/or the fixed surface area increases. It can be noted that the ratios for fixed surface area are very smaller than those for fixed volume. It means physically that applying the optimum dimensions for fixed surface area probably seems to be needed for a particular place such as the space in which a relatively long fin cannot be installed.

In the case of fixed surface area, the variations of the optimum heat loss and effectiveness as a function of M are presented in Fig. 13. The optimum heat loss increases linearly as M increases from 0.01 to 0.1. It shows that the corresponding optimum effectiveness is relatively very low for the given range of M . It is because the optimum fin length is very short and

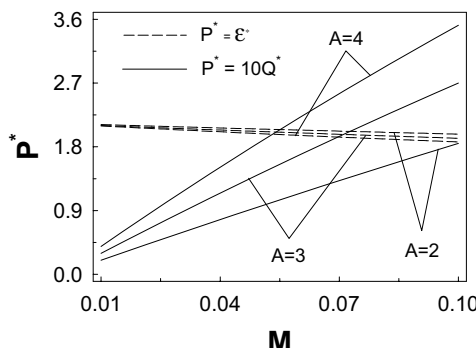


Fig. 13. Optimum heat loss and fin effectiveness vs. the convection characteristic number for fixed surface areas ($\xi = 0.5$, $L_b = 0.1$).

the optimum base height is high, as already shown in Fig. 12 and Table 3.

4. Conclusions

From the optimization of a reversed trapezoidal fin using a two-dimensional analytic method, the following conclusions can be drawn. First, for the fixed fin volume,

(1) The maximum heat loss in the practical fin length does not exist when the fin base thickness, the ratio of fin tip height to base height and the fin volume are larger than the certain values.

(2) Both the optimum heat loss and the corresponding fin effectiveness decrease with the increase of the fin base thickness.

(3) Both the optimum heat loss and the optimum fin length increase with the increase of the value of fin shape factor.

(4) Even though the optimum heat loss increases, the corresponding optimum fin effectiveness decreases as the fin volume increases. It is because the increasing rate of the optimum fin length is less than that of the optimum fin base height with the increase of the fin volume.

And in the case of fixed fin surface area,

(5) The fin length for the optimum heat loss is very short so optimum dimensions for the fixed surface area are probably needed for a particular place such as the space in which a relatively long fin cannot be installed.

Nomenclature

a : Fin surface area [m^2]

- A : Dimensionless fin surface area, $a/(l_c l_w)$
- h : Heat transfer coefficient over the fin [$W/m^2 \text{ } ^\circ\text{C}$]
- k : Thermal conductivity of the fin material [$W/m \text{ } ^\circ\text{C}$]
- l_b : Fin base thickness [m]
- L_b : Dimensionless fin base thickness, l_b/l_c
- l_c : Characteristic length [m]
- l_e : Fin tip length [m]
- L_e : Dimensionless fin tip length, l_e/l_c
- l_h : One half fin base height [m]
- L_h : Dimensionless one half fin base height, l_h/l_c
- l_w : Fin width [m]
- q : Heat loss from the fin [W]
- Q : Dimensionless heat loss from the fin, $q/(kl_w \varphi_i)$
- q_w : Heat loss from the bare wall [W]
- Q_w : Dimensionless heat loss from the bare wall, $q_w/(kl_w \varphi_i)$
- s : Fin lateral surface slope, $\{(1-\xi)l_h\}/(l_e-l_b)$
- T : Fin temperature [$^\circ\text{C}$]
- T_h : Fin base temperature [$^\circ\text{C}$]
- T_i : Inside wall temperature [$^\circ\text{C}$]
- T_∞ : Ambient temperature [$^\circ\text{C}$]
- v : Fin volume [m^3]
- V : Dimensionless fin volume, $v/(l_c^2 \cdot l_w)$
- x : Length directional variable [m]
- X : Dimensionless length directional variable, x/l_c
- y : Height directional variable [m]
- Y : Dimensionless height directional variable, y/l_c

Greek symbol

- ε : Fin effectiveness
- φ_i : Adjusted inside wall temperature [$^\circ\text{C}$], $(T_i - T_\infty)$
- λ_n : Eigenvalues ($n = 1, 2, 3, \dots$)
- θ : Dimensionless temperature, $(T - T_\infty)/(T_i - T_\infty)$
- ξ : Fin shape factor, ($0 \leq \xi \leq 1$)

Subscript

- b : Fin base
- c : Characteristic
- e : Fin tip
- h : Fin height at the base
- i : Inside wall
- w : Outside bare wall or width
- ∞ : Surrounding

Superscript

- * : Optimum

References

- [1] A. K. Sen and S. Trinh, An exact solution for the rate of heat transfer from a rectangular fin governed by a power law-type temperature dependence, *ASME J. of Heat Transfer* 108 (1986) 457-459.
- [2] S. Abrate and P. Newnham, Finite element analysis of triangular fins attached to a thick wall, *Computers and Structures* 57 (6) (1995) 945-957.
- [3] S. Sikka and M. Iqbal, Temperature distribution and effectiveness of a two-dimensional radiating and convecting circular fin, *AIAA Journal* 8 (1) (1970) 101-106.
- [4] R. H. Yeh, An analytical study of the optimum dimensions of rectangular fins and cylindrical pin fins, *Int. J. of Heat and Mass Transfer* 40 (15) (1997) 3607-3615.
- [5] L. T. Yu and C. K. Chen, Optimization of circular fins with variable thermal parameters, *Journal of The Franklin Institute* 336 (B) (1999) 77-95.
- [6] H. S. Kang and D. C. Look Jr., Optimization of a thermally asymmetric convective and radiating annular fin, *Heat Transfer Engineering* 28 (4) (2007) 310-320.
- [7] A. Bejan and M. Almogbel, Constructal T-shaped fins, *Int. J. of Heat and Mass Transfer* 43 (2000) 2101-2115.
- [8] B. Kundu and P. K. Das, Performance analysis and optimization of elliptical fins circumscribing a circular tube, *Int. J. of Heat and Mass Transfer* 50 (2007) 173-180.
- [9] D. C. Look, Separation of variables on a triangular geometry, *Q. J. appl. Math.* 1 (1992) 141-148.
- [10] H. S. Kang and D. C. Look Jr., A comparison of four solution methods for the analysis of a trapezoidal fin, *KSME International Journal* 13 (6) (1999) 487-495.
- [11] C. H. Cho., Y. M. Han and H. S. Kang, Comparison between analytic method and experimentation on the trapezoidal fin, *Journal of Industrial Technology* 25 (A) (2005) 75-80.
- [12] H. S. Kang, Optimization of a reversed trapezoidal fin, *Journal of KSME(B)* 30 (10) (2006) 987-995.